POLITECNICO DI TORINO
Repository ISTITUZIONALE

Thermal Dynamics of Settling Inertial Particles in a Stably Stratified Turbulent Flow

Original
Thermal Dynamics of Settling Inertial Particles in a Stably Stratified Turbulent Flow / Zandi Pour, Hamid Reza; Iovieno, Michele. - ELETTRONICO. - (2025), pp. 1-8. (12th International Conference on Heat Transfer and Fluid Flow (HTFF 2025) Paris (FRA) August 19-21, 2025) [10.11159/htff25.167].

Availability:
This version is available at: 11583/3003219 since: 2025-09-20T16:41:54Z

Publisher:
INTERNATIONAL ASET INC.

Published
DOI:10.11159/htff25.167

Terms of use:

This article is made available under terms and conditions as specified in the corresponding bibliographic description in the repository

Publisher copyright

(Article begins on next page)

26 April 2026

Proceedings of the 11th World Congress on Mechanical, Chemical, and Material Engineering (MCM'25)
Paris, France - August, 2025
Paper No. HTFF 167
DOI: 10.11159/htff25.167

Thermal Dynamics of Settling Inertial Particles in a Stably Stratified Turbulent Flow

Hamid Reza Zandi Pour[1,2], Michele Iovieno[2]
[1]Dipartimento di Fisica and INFN - Università degli Studi di Torino
Via Pietro Giuria, 1, 10125 Torino, Italy
[2]Dipartimento di Ingegneria Meccanica e Aerospaziale, Politecnico di Torino
Corso Duca degli Abruzzi 24, 10129 Torino, Italy
hamid.zandipour@polito.it; michele.iovieno@polito.it

Abstract - The effect of settling inertial particles in forced homogeneous and isotropic turbulence, within the Boussinesq approximation, has been studied. An Eulerian-Lagrangian point-particle direct numerical simulation (DNS) approach is employed to simulate a diverse range of particle inertia and settling parameters. We investigate the impact of the particle settling parameter, which can reach values up to 1, as well as the influence of inertia on flow statistics. Our observations indicate that the settling parameter alters the fluid-particle velocity and temperature difference moments, with the effect becoming more pronounced as both particle inertia and thermal inertia increase. All statistics have been compared to the case in which particle settling is neglected. Results are presented for a diverse range of particle Stokes numbers, from 0.1 to 4, with a thermal Stokes number to Stokes number ratio of 6.24, at a Taylor microscale Reynolds number of 128, and a Richardson number of 0.25.

***Keywords*:** heat transfer, fluid-particle thermal interaction, settling particles, buoyancy, turbulent mixing

1. Introduction

The suspension of inertial particles in thermally stratified turbulent flows represents a highly complex and frequently encountered scenario in both natural phenomena and industrial applications. Regardless of whether the stratification of the carrier flow is stable or unstable, particle settling must be properly understood in order to complete the picture of fluid–particle interaction, alongside the roles of particle inertia and thermal inertia. Despite its significance—impacting phenomena such as turbulence sampling by particles, preferential concentration, caustics and thermal caustics, scattering, and non-local history effects—settling remains an open problem. An increasing number of studies are dedicated to investigating various aspects of this issue (e.g. [1], [2]); however, many works continue to neglect it, either for the sake of simplifying the analysis or due to limitations in numerical simulations. The thermal interaction between the fluid and settling particles has recently been investigated by Li et al. [3], who demonstrated that settling disrupts Lagrangian correlations and modifies the occurrence of thermal caustics—an ubiquitous phenomenon for particles with finite thermal inertia arising as a consequence of caustic formation [4]. However, the effect of settling in a thermally stratified flow has yet to be addressed. In such cases, where the flow is thermally stratified, the interaction among buoyancy, settling, and turbulence further increases the intrinsic complexity of fluid–particle dynamics, which is already non-trivial. Particulate turbulent flows remain significantly more complex than single-phase flows and, within the context of turbulence research, are still relatively immature. For instance, we have recently examined fluid–particle thermal interaction within a time-evolving, shearless thermal mixing layer in a collisionless regime [5, 6], as well as in a collisional regime [7], though gravitational effects were not considered. More recently, Grace et al. [8] investigated the influence of settling in stratified channel flows, while Pan et al. [9] explored the settling of inertial particles in a mixed-convection, wall-bounded turbulent flow subject to unstable stratification. Gravity is also often absent from studies addressing fluid–particle thermal interactions using the point-particle approach, which is valid for sub-Kolmogorov-scale particles. This omission is seen in both wall-bounded flows [10-13] and unbounded configurations [14-16]. To advance understanding of the fundamental physics underlying fluid–particle interactions in turbulent flows, it is essential to account for the role of gravity. The presence of gravity introduces anisotropy and may either counteract or enhance turbulent transport mechanisms. In a recent study, Li et al. [3] analysed the effects of gravity on inertial particles in homogeneous isotropic turbulence. Their results show that gravity alters particle trajectories, weakens non-local history effects—particularly for high-inertia particles—and

affects clustering behaviour. Notably, they found that gravity increases the efficiency of particle heat transfer by changing the way particles sample fluid temperature gradients.

In this paper, we extend previous studies on settling inertial particles to the case where the buoyancy term is also included in the fluid equations. This allows us to examine a more realistic scenario in which the interaction between settling inertial particles and a stably stratified flow can be studied in depth. The aim of the present work is to elucidate how gravitational settling affects the dynamical and thermal interactions of inertial particles with turbulence. To investigate this, we perform direct numerical simulations (DNS) in a stably stratified flow subject to homogeneous forcing of the velocity field and an imposed mean temperature gradient. We analyse the role of the particle Stokes number—quantifying particle inertia—and a gravitational parameter, defined as the inverse of the Froude number. All other non-dimensional parameters, including the Reynolds number, Richardson number, and Prandtl number, are held constant so that the particles experience an identical turbulent environment. All simulations in this study are conducted in the thermally and dynamically one-way coupling regime, with a focus on the effects of particle settling at a low particle volume fraction. Following a brief presentation of the governing equations for fluid and particle dynamics in Section 2—expressed in dimensionless form along with the numerical methodology—we present, in Section 3, preliminary results concerning the statistics of the relative velocity between the particles and the surrounding fluid (commonly referred to as the 'slip' velocity), as well as the temperature difference between the particles and the fluid.

2. Physical model

2.1. Governing equations

To investigate the thermal and dynamical interaction between stratified turbulence and settling inertial particles, the Boussinesq approximation is adopted. The governing equations are non-dimensionalised using a characteristic length scale L_0, velocity scale U_0, and temperature difference ΔT, with the vertical direction aligned along the third coordinate axis. Under these assumptions, the dimensionless Navier–Stokes equations for the carrier fluid read:

$$\partial_j u_j = 0, \tag{1}$$

$$\partial_t u_i + u_j \partial_j u_i = -\partial_i p + 1/Re\, \partial_j \partial_j u_i + Ri\theta\, \delta_{i3} + f_{u,i}, \tag{2}$$

$$\partial_t \theta + u_j \partial_j \theta = 1/RePr\, \partial_j \partial_j \theta - u_3, \tag{3}$$

where $p(t,x)$, $u(t,x)$, and $\theta(t,x)$ denote the fluid pressure, velocity, and temperature deviation from the static profile, respectively. The Reynolds, Richardson, and Prandtl number are defined as $Re = U_0 L_0/\nu$, $Pr = \nu/\kappa$, and $Pr = \nu/\kappa$ where ν and κ are the kinematic viscosity and thermal diffusivity of the fluid, g is the gravitational acceleration, and α_T is the thermal expansion coefficient. The forcing term $f_{u,i}$ is used to sustain statistically stationary turbulence. The buoyancy term $Ri\theta\,\delta_{i,3}$ couples momentum and temperature fluctuations due to the stable stratification ($Ri > 0$). The motion of inertial point-particles, whose density is much larger than that of the fluid, is described by the following non-dimensional equations, which are a simplified form of the Maxey-Riley equations:

$$\frac{d}{dt}\begin{pmatrix} X_{p,i}(t) \\ V_{p,i}(t) \\ \theta_p(t) \end{pmatrix} = \begin{bmatrix} 0 & 1 & 0 \\ 0 & -1/St & 0 \\ 0 & -\delta_{i3} & -1/St_\vartheta \end{bmatrix} \begin{pmatrix} X_{p,i}(t) \\ V_{p,i}(t) \\ \theta_p(t) \end{pmatrix} + \begin{bmatrix} 0 \\ 1/St\, u(t, X_p) - 1/Fr^2\, \delta_{i3} \\ 1/St_\vartheta\, \theta(t, X_p) \end{bmatrix}, \tag{4}$$

$$\tag{5}$$

$$\tag{6}$$

where $X_p(t)$, $V_p(t)$, and $\theta_p(t)$ denote the position, velocity, and temperature deviation from the static profile of the $p-th$; $u(t, X_p)$ and $\theta(t, X_p)$ are the fluid velocity and temperature sampled at the particle position. The particle Stokes number $St = \tau_v/T_0$ and thermal Stokes number $St_\vartheta = \tau_\vartheta/T_0$ represent the dimensionless momentum and thermal relaxation times, respectively, defined as

$$\tau_v = \frac{2}{9}\frac{\rho_p}{\rho_f}\frac{R^2}{\nu}, \tau_\vartheta = \frac{1}{3}\frac{\rho_p c_{pp}}{\rho_f c_{pf}}\frac{R^2}{\kappa}, \tag{7}$$

where R is the particle radius, ρ_p and $c_{pp}$are the particle density and specific heat capacity at constant pressure, while ρ_f and $c_{pf}$are the fluid density and specific heat capacity at constant pressure, normalized with the reference time scale of the flow L_0/U_0. The particle volume fraction is assumed to be sufficiently low such that particle–fluid interactions are restricted to one-way coupling. At these dilute concentrations, particle–particle collisions are also negligible and can be ignored without affecting the temperature statistics, as shown in [7].

Table 1: Dimensionless flow parameters.

Taylor microscale Reynolds number	Re_λ	128
Prandtl number	Pr	1
Richardson number	Ri	0.25
Taylor microscale	λ	0.32
Integral length scale	l	0.91
Kinematic viscosity	ν	1.668×10^{-3}
RMS velocity fluctuations	u_{rms}	0.67
RMS temperature fluctuations	θ_{rms}	0.81
Forced wavenumber	κ_f	$\sqrt{3}$
Dissipation rate	ε	0.13
Kolmogorov length scale	η	0.014
Kolmogorov time scale	τ_η	0.113
Kolmogorov velocity scale	u_η	0.121
Eddy turnover time	τ	1.35
Number of Fourier modes	$N_1 = N_2 = N_3$	512
Resolution	κ_{max}/η	3.57
Time step	Δt	1×10^{-3}
Particle volume fraction	φ	4×10^{-4}
Density ratio	ρ_p/ρ_f	10^3
Thermal-to-momentum relaxation time ratio	St_ϑ/St	6.24
Kolmogorov scale Stokes number	St_η	0.1; 0.2; 0.3; 0.5; 0.7; 0.8; 0.9; 1; 1.2; 1.5; 2; 2.5; 3; 4
Particle gravity parameter (inverse Froude number sq)	$1/Fr^2$	0; 0.1; 0.2; 0.5; 1

Figure 1: Mean fluid velocity at particle position (a); mean particle-fluid temperature difference (b).

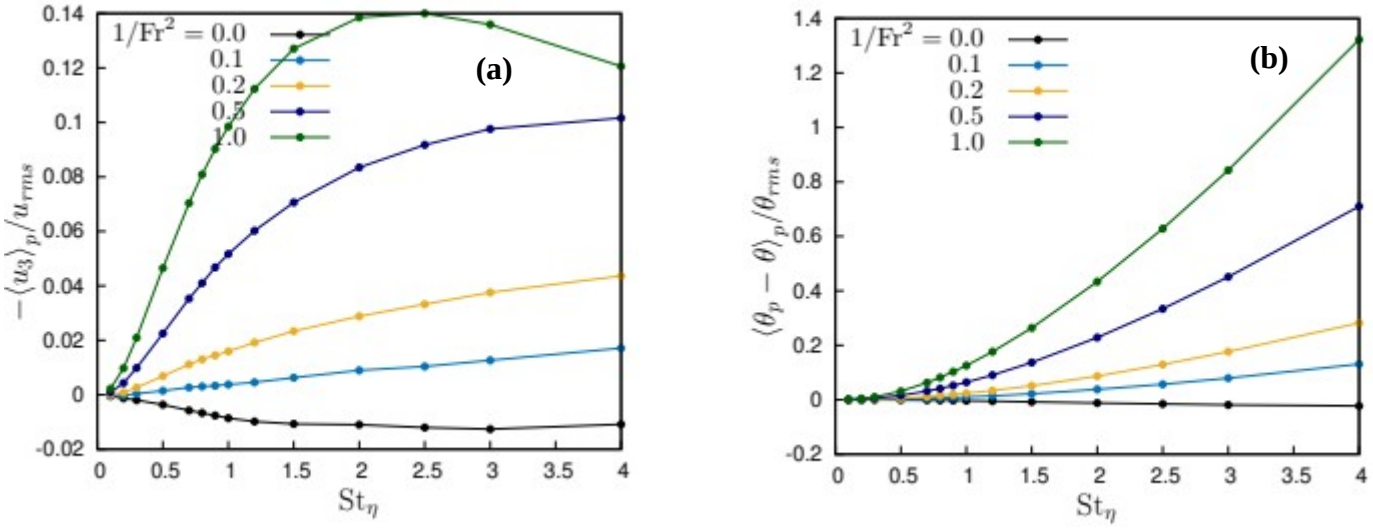

2.2. Flow configuration and numerical method

The governing equations (1)–(3) are solved within a cubic domain of side length L, employing periodic boundary conditions on all faces. Particles exiting the domain re-enter from the opposite side, maintaining their velocity and temperature. The non-dimensionalisation of the equations is based on the characteristic length scale $L_0 = L/(2\pi)$, a velocity scale defined from the energy injection rate ε_f of the forcing term, $U_0 = (6\varepsilon_f / L_0)^{1/3}$, and a temperature scale $\Delta T = \Gamma L_0$ where Γ denotes the imposed mean temperature gradient. As is customary in homogeneous turbulent flows, results will be presented using the Taylor microscale as the reference length scale for defining the Reynolds number, as it more accurately captures the local dynamics of the turbulence. The Kolmogorov time scale, $\tau = (\nu/\varepsilon)^{1/2}$, is used as the reference time scale for particles, since it corresponds to the smallest temporal scale of the flow, to which particles predominantly respond. The relevant flow parameters for the simulations are summarised in Table 1. A fully dealiased pseudo-spectral method (using the $3/2$ rule) is employed for the spatial discretisation of the fluid equations (1)–(3). The external forcing term f_u is implemented in Fourier space and defined as

$$\widehat{f_{u,i}}(t,\kappa) = \varepsilon_f \frac{\hat{u}_i(t,\kappa)}{\sum_{\|\kappa\|=\kappa_f} \| \hat{u}_i(t,\kappa) \|^2} \cdot \delta(\|\kappa\| - \kappa_f), \tag{8}$$

where ε_f is the prescribed energy injection rate (set to $1/6$ in dimensionless units), and κ_f is the forced wavenumber. Interpolation of fluid velocity and temperature at particle positions is carried out using a recently developed numerical method [17,18], which relies on non-uniform fast Fourier transforms combined with a fourth-order B-spline basis. Time integration of both the fluid equations (1)–(3) and the particle equations (4)–(6) is performed using a second-order exponential integrator. Statistics are computed over several large-eddy turnover times, ensuring statistical convergence.

Figure 2: Variance of particle-fluid temperature (a) and velocity difference (b).

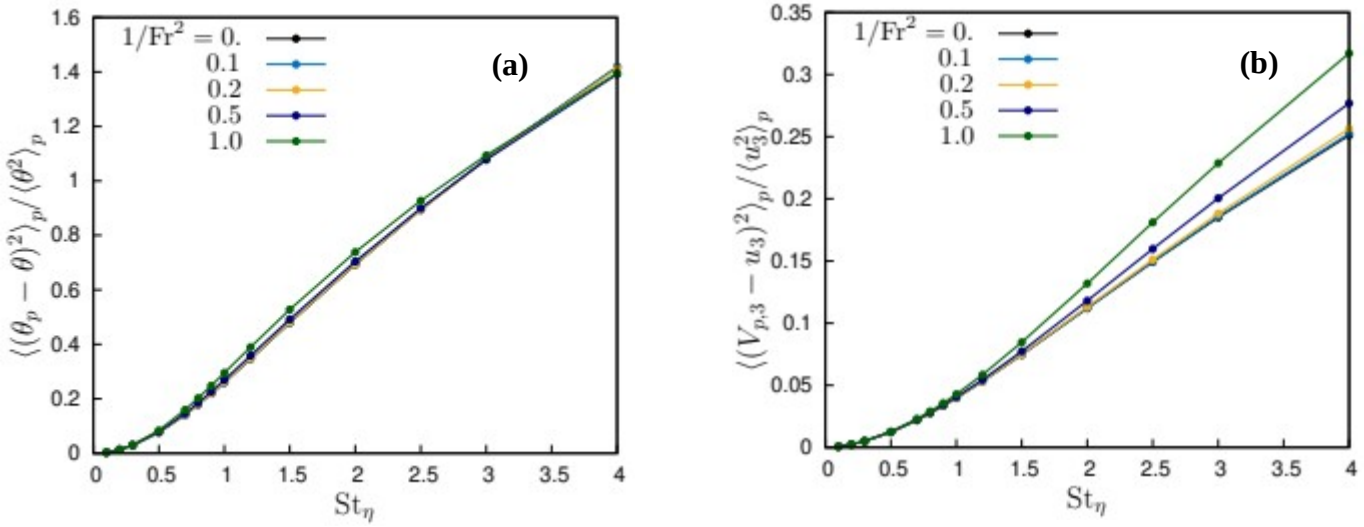

Figure 3: Skweness of particle-fluid temperature (a) and velocity difference (b). Data in absence of settling, $Fr^2 \to \infty$ are shown as a measure of statistical accuracy.

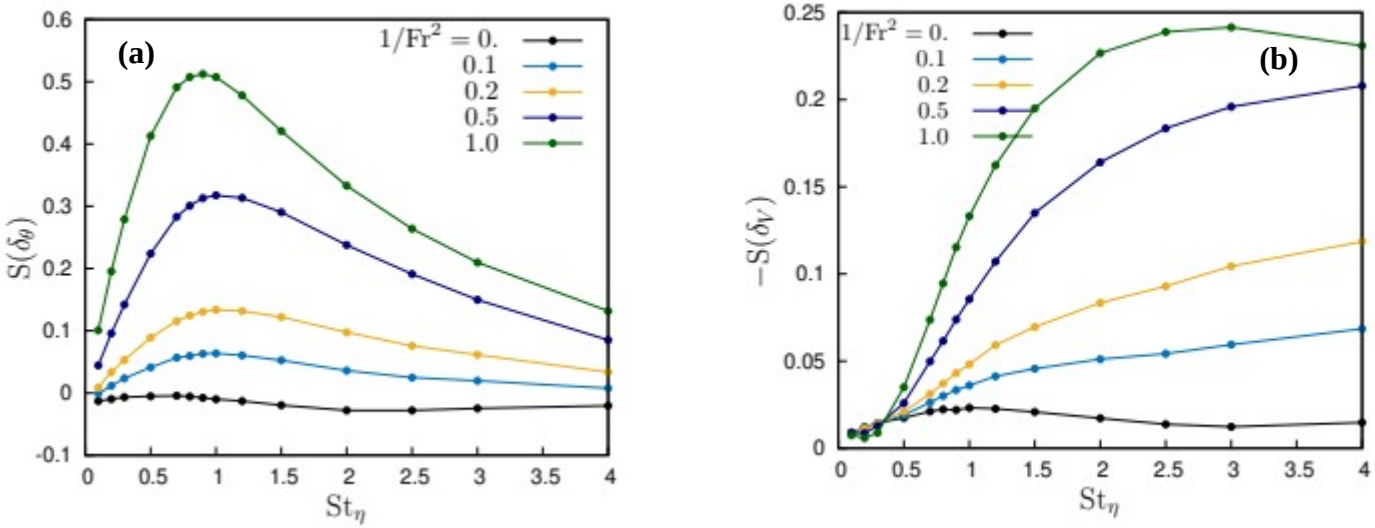

Figure 4: Kurtosis of particle-fluid temperature (a) and velocity difference (b).

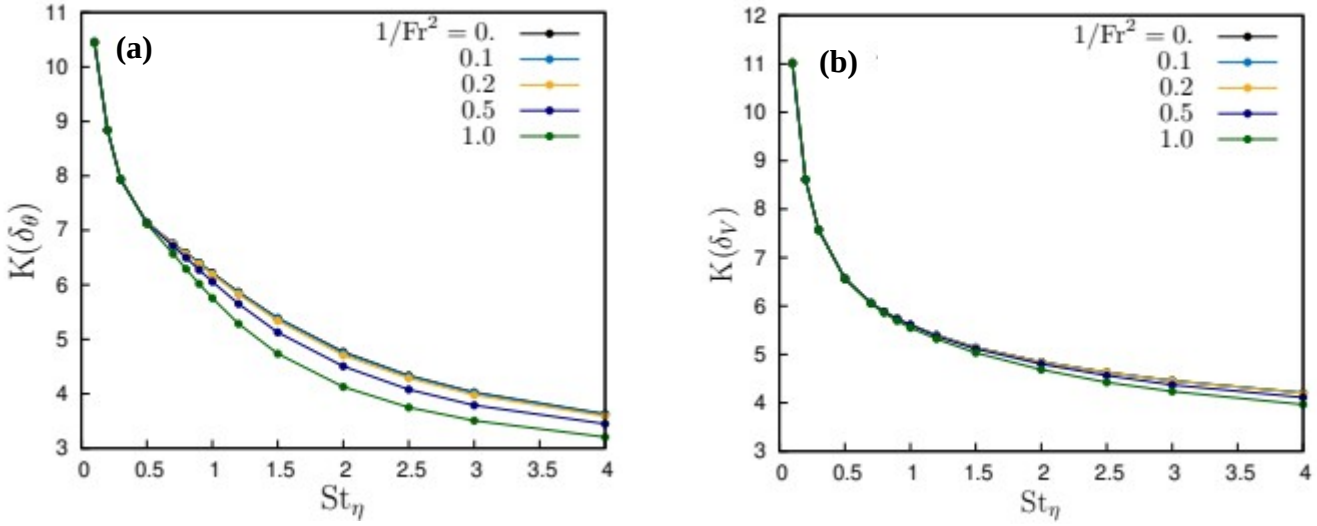

3. Results

We present preliminary single-point statistics on the vertical velocity and temperature differences between fluid and particles at low to moderate gravitational settling (Froude numbers $Fr>1$). In all simulations, the Reynolds and Richardson numbers are fixed, while the Stokes and inverse Froude numbers are varied to assess their impact on fluid-particle thermal interaction.

Inertial particles are known to preferentially sample regions of strong temperature gradients, such as thermal fronts, due to their tendency to concentrate in high-strain regions of turbulence [14]. However, gravity-induced settling reduces this preferential concentration, weakening both caustic and thermal caustic formation[3]. Gravitational settling reduces the interaction time between particles and turbulent eddies, hindering particles' ability to sample high-strain regions of the flow [1]. This, in turn, alters the fluid-particle thermal interaction, as those high-strain regions are also temperature fronts [14] thus reducing thermal caustics formation and their overall impact on particle statistics. Although $\langle u_i \rangle = \langle \theta \rangle = 0$ the gravity-induced drift results in non-zero mean particle velocity and temperature. From equations (5) and (6), the average vertical velocity and temperature of particles are $\langle v_{p,3} \rangle_p = \langle u_3 \rangle_p - St/Fr^2$, and $\langle \theta_p \rangle_p = \langle \theta \rangle_p - St_\vartheta \langle u_3 \rangle_p - St_\vartheta St/Fr^2$ highlighting the role of preferential sampling even in weakly stratified, settling environments.

This effect is shown in figure 1(a), where the mean fluid velocity at particle positions is always negative. Without turbulence, particles would settle with a velocity equal to $-St/Fr^2$, but turbulent preferential sweeping can either increase or decrease this settling velocity through $\langle u_3 \rangle_p$. For particles with low to moderate Stokes numbers ($St \sim 0.5$), turbulence enhances settling velocity, particularly as the Froude number decreases, through this preferential sweeping mechanism. While Ireland et al. [1] observed this effect diminishing for $St \gtrsim 1$, and eventually vanishing when $St \sim O(10)$, we find it persists in our simulations until the Froude number reaches unity. This effect could peak at a Stokes number that decreases as the Froude number decreases, but further investigation at higher Stokes numbers is needed. Moreover, it should be observed that in [1] and [3] the Froude number is much smaller ($1/Fr^2 = 24$ in [1] and $Fr>10$ in [3]) than in this work. However, at smaller Froude numbers, gravitational settling increases, and the validity of the linear Stokes drag approximation in equation (5) becomes questionable.

Since velocity and temperature correlations are negatively correlated, a negative u_3 is associated with a positive θ. Therefore, a larger settling velocity has the effect of further intensifying the temperature difference between the particles and surrounding fluid (figure 1(b)), thus enhancing heat transfer between fluid and particles.

The even moments of the relative velocity and temperature differences are not significantly modified by the Froude number. From equations (5)–(6), one deduces that $\langle V'^2_{p,3}\rangle_p = \langle u'_3 V'_{p,3}\rangle_p$ and $\langle \theta'^2_p\rangle_p = \langle \theta'_p \theta'\rangle_p - St_\vartheta \langle V'_{p,3}\theta'\rangle_p$, so that the variances of the velocity and temperature differences between particles and fluid are

$$\left\langle \left(u'_3 - V'_{p,3}\right)^2 \right\rangle_p = \left\langle u'^2_3 \right\rangle_p - \left\langle u'_3 V'_{p,3}\right\rangle_p,$$
$$\left\langle \left(\theta' - \theta'_p\right)^2 \right\rangle_p = \left\langle \theta' \right\rangle^2_p - \left\langle \theta' \theta'_p \right\rangle_p - St_\vartheta \left\langle V'_{p,3}\theta'_p \right\rangle_p.$$

Gravitational settling progressively decouples particle and fluid trajectories, thus reducing correlations and, as a consequence, increasing the variance of their differences. For any given Froude number, this effect is most appreciable for high Stokes number particles, since they have the largest velocity difference with respect to the surrounding fluid, and becomes more pronounced when at $1/Fr^2 = 1$, when gravity begins to act over the eddy turnover timescales.
The role of settling in modulating the relative temperature variance is more indirect, and temperature variance responds more subtly. The decoupling between fluid and particles is balanced by the turbulent sweeping of particles into regions of negative u_3 and positive θ, an effect more pronounced when $St \gtrsim 1$. This increases the correlation $\langle \theta'_p \theta' \rangle_p$ as particles preferentially sample descending plumes. However, the negative correlation $\langle V'_{p,3}\theta_p' \rangle_p$, amplified by the thermal Stokes number, dominates, marginally increasing the variance of the temperature difference, especially at higher inverse Froude numbers (figure 2).

The variance of the particle-fluid velocity and temperature differences cannot be scaled according to the model by Ireland et al. [1] since that model assumes $St/Fr^2 \gg u'/u_\eta \sim Re_\lambda^{1/2}$, a scenario applicable only at very small Froude numbers where gravity dominates the particle dynamics overcoming the Stokes drag which binds particles to fluid motion. In our simulations, Froude number is larger than one and gravity has a minor impact on the velocity variance, producing significant increases only for large Stokes numbers. The effect on particle temperature variance is even smaller (figure 2). We also note that, with $St_\vartheta/St \approx 6$, the thermal inertia filtering effect prevails at all Stokes numbers, except the smallest ones. However, settling shifts the tails of the velocity and temperature difference distributions, with a consistent tendency toward negative velocity and positive temperature fluctuations (figure 3), even though the relatively small settling velocity (parameter $Sv = St/Fr^2$, which is always below 4) does not significantly alter the intermittency of relative velocity and temperature, as indicated by their kurtosis (figure 4). The largest skewness is obtained by particles who experience the more intense sweeping by turbulence. Conditional averages and cross-correlation between velocity and temperature with a time lag could highlight the role of inertia, as well as simulations with different St_ϑ/St ratios.

It is important to note that the simulations by Li et al. [3]and Ireland et al. [1] correspond to the case $Ri = 0$, where particles settle in an isotropic turbulent field. In contrast, our setup includes stable stratification, even if a relatively weak one, where buoyancy tends to suppress vertical motions, introducing flow anisotropy. Despite a relatively low Richardson number ($Ri = 0.25$), anisotropy remains mild, with $\langle u'^2_3 \rangle / \langle u'^2_1 \rangle \approx 0.9$. Higher Richardson numbers may further reduce the role of turbulence in particle dynamics by suppressing vertical motion, thus weakening the role of preferential sweeping.

4. Conclusion

In this study, we investigated some aspects of the thermal interaction between fluid particles in the presence of a stable stratification. While gravity, through stratification, removes isotropy, the different action of gravity of fluid and particles modifies their interaction, making particles leave high-strain regions, modulating the preferential concentration on high-strain regions with a preferential sampling of downward flow regions, which produces a preferential sweeping effect. The result is a large mean temperature drift, with the particles remaining significantly warmer than the fluid, which increases as the inverse Froude number increases. This effect skews the temperature distribution of the particles, suppressing the negative tail of the probability density. Anyway, at large Stokes number, the inertial filtering effect still prevails. Further insight could be obtained by analysing the probability density functions of the invariants and the alignment of the fluid and particle temperature gradients with the eigenvectors of the strain rate tensor In future works, it will be important to

consider the coupling effects on temperature and velocity correlation, which determine the heat transfer, and the effect of two-way coupling between particles and fluid, and to analyse two-point statistics to look at a the scale dependence of settling on thermal interaction, as well as the effect of a larger Richardson number.

Acknowledgements

The authors acknowledge the CINECA award IsCc4_GSPLF, HP10CP6FB6, under the ISCRA initiative, for the availability of high-performance computing resources and support.

References

[1] P. J. Ireland, A. D. Bragg, and L. R. Collins, "The effect of Reynolds number on inertial particle dynamics in isotropic turbulence. Part 2. Simulations with gravitational effects," Journal of Fluid Mechanics, vol. 796, pp. 659—-711, 2016.

[2] A. D. Bragg, D. H. Richter, and G. Wang, "Settling strongly modifies particle concentrations in wall-bounded turbulent flows even when the settling parameter is asymptotically small," Phys. Rev. Fluids, vol. 6, p. 124301, Dec 2021.

[3] S. Li, Z. Cui, C. Xu, and L. Zhao, "Temperature statistics of settling particles in homogeneous isotropic turbulence," International Journal of Heat and Mass Transfer, vol. 228, p. 125555, 2024.

[4] H. R. Zandi Pour and M. Iovieno, "On the formation of thermal caustics in turbulent particle-laden flows," Physics of Fluids, vol. 36, p. 121711, 12 2024.

[5] H. R. Zandi Pour and M. Iovieno, "Heat transfer in a non-isothermal collisionless turbulent particle-laden flow," Fluids, vol. 7, no. 11, p. 345, 2022.

[6] H. R. Zandi Pour and M. Iovieno, "The role of particle inertia and thermal inertia in heat transfer in a non-isothermal particle-laden turbulent flow," Fluids, vol. 9, no. 1, 2024.

[7] H. R. Zandi Pour and M. Iovieno, "The impact of collisions on heat transfer in a particle-laden shearless turbulent flow," Journal of Fluid Flow, Heat and Mass Transfer, vol. 10, pp. 140–149, 2023.

[8] A. P. Grace and D. Richter, "Multi-scale interactions in turbulent mixed convection drive efficient transport of Lagrangian particles," Journal of Fluid Mechanics, vol. 1008, p. A30, 2025.

[9] M. Pan, L. Shen, Q. Zhou, and Y. Dong, "Particle transport and turbulence modification in unstably stratified mixed convection within a horizontal channel," International Journal of Heat and Mass Transfer, vol. 236, p. 126377, 2025.

[10] F. Zonta, C. Marchioli, and A. Soldati, "Direct numerical simulation of turbulent heat transfer modulation in micro-dispersed channel flow," Acta Mechanica, vol. 195, pp. 305–326, 2008.

[11] J. G. M. Kuerten, C. W. M. van der Geld, and B. J. Geurts, "Turbulence modification and heat transfer enhancement by inertial particles in turbulent channel flow," Phys. Fluids, vol. 23, no. 12, p. 123301, 2011.

[12] F. Rousta and B. Lessani, "Near-wall heat transfer of solid particles in particle-laden turbulent flows," International Communications in Heat and Mass Transfer, vol. 112, p. 104475, 2020.

[13] D. Zaza and M. Iovieno, "Mixed convection in turbulent particle-laden channel flow at $Re_\tau = 180$," Journal of Physics: Conference Series, vol. 2685, no. 1, p. 012003, 2024.

[14] J. Béc, H. Homann, and G. Krstulovic, "Clustering, fronts, and heat transfer in turbulent suspensions of heavy particles," Physical Review Letters, vol. 112, p. 234503, 2014.

[15] M. Carbone, A. D. Bragg, and M. Iovieno, "Multiscale fluid-particle thermal interaction in isotropic turbulence," J. Fluid Mech., vol. 881, pp. 679–721, 2019.

[16] I. Saito, T. Watanabe, and T. Gotoh, "Modulation of fluid temperature fluctuations by particles in turbulence," J. Fluid Mech., vol. 931, p. A6, 2022.

[17] M. Carbone and M. Iovieno, "Application of the non-uniform Fast Fourier Transform to the Direct Numerical Simulation of two-way coupled turbulent flows," WIT Trans. Eng. Sci., vol. 120, pp. 237–248, 2018.

[18] M. Carbone and M. Iovieno, "Accurate direct numerical simulation of two-way coupled particle-laden flows through the nonuniform Fast Fourier Transform," Int. J. Safety and Sec. Eng., vol. 10, no. 2, pp. 191–200, 2020.